NeuroImage 56 (2011) 212–219

Contents lists available at ScienceDirect

NeuroImage

journal homepage: www.elsevier.com/locate/ynimg

# Automated hippocampal shape analysis predicts the onset of dementia in mild cognitive impairment

Sergi G. Costafreda [a,*,1], Ivo D. Dinov [b,1], Zhuowen Tu [b,1], Yonggang Shi [b,1], Cheng-Yi Liu [b,1], Iwona Kloszewska [c,1], Patrizia Mecocci [d,1], Hilkka Soininen [e,1], Magda Tsolaki [f,1], Bruno Vellas [g,1], Lars-Olof Wahlund [h,1], Christian Spenger [h,1], Arthur W. Toga [b,1], Simon Lovestone [a,1], Andrew Simmons [a,1]

[a] NIHR Biomedical Research Centre for Mental Health at South London and Maudsley NHS Foundation Trust and King's College London, London, UK
[b] Laboratory of NeuroImaging, UCLA, Los Angeles, CA, USA
[c] Department of Old Age Psychiatry and Psychotic Disorders, Medical University of Lodz, Poland
[d] Institute of Gerontology and Geriatrics, University of Perugia, Perugia, Italy
[e] Department of Neurology, University of Eastern Finland and Kuopio University Hospital, Kuopio, Finland
[f] Department of Neurology, Aristotle University, Thessaloniki, Greece
[g] Toulouse Gérontopôle University Hospital, Université Paul Sabatier, INSERM U 558, France
[h] Department of Clinical Science, Intervention and Technology, Karolinska Institutet, Stockholm, Sweden

ARTICLE INFO

*Article history:*
Received 2 September 2010
Revised 14 January 2011
Accepted 17 January 2011
Available online 25 January 2011

*Keywords:*
Neuroimaging
Hippocampus
Prognosis
Automated methods
Alzheimer's disease
Mild cognitive impairment

ABSTRACT

The hippocampus is involved at the onset of the neuropathological pathways leading to Alzheimer's disease (AD). Individuals with mild cognitive impairment (MCI) are at increased risk of AD. Hippocampal volume has been shown to predict which MCI subjects will convert to AD. Our aim in the present study was to produce a fully automated prognostic procedure, scalable to high throughput clinical and research applications, for the prediction of MCI conversion to AD using 3D hippocampal morphology. We used an automated analysis for the extraction and mapping of the hippocampus from structural magnetic resonance scans to extract 3D hippocampal shape morphology, and we then applied machine learning classification to predict conversion from MCI to AD. We investigated the accuracy of prediction in 103 MCI subjects (mean age 74.1 years) from the longitudinal AddNeuroMed study. Our model correctly predicted MCI conversion to dementia within a year at an accuracy of 80% (sensitivity 77%, specificity 80%), a performance which is competitive with previous predictive models dependent on manual measurements. Categorization of MCI subjects based on hippocampal morphology revealed more rapid cognitive deterioration in MMSE scores ($p<0.01$) and CERAD verbal memory ($p<0.01$) in those subjects who were predicted to develop dementia relative to those predicted to remain stable. The pattern of atrophy associated with increased risk of conversion demonstrated initial degeneration in the anterior part of the cornus ammonis 1 (CA1) hippocampal subregion. We conclude that automated shape analysis generates sensitive measurements of early neurodegeneration which predates the onset of dementia and thus provides a prognostic biomarker for conversion of MCI to AD.



## Introduction

Mild cognitive impairment (MCI) refers to a clinical syndrome characterized by significant cognitive impairments which are beyond normal for healthy adults but not sufficient to meet clinical criteria for Alzheimer's disease (AD). The rate of conversion from MCI to overt dementia is substantial, at 10%–15% per year, the majority of which is AD (Petersen et al., 2001). As the clinical features of AD are the outcome of at least a decade of progressive neuropathological changes (Nelson et al., 2009; Jack et al., 2010), structural neuroimaging has shown potential in predicting the onset of AD in MCI subjects (Jack et al., 1999; Killiany et al., 2002; Teipel et al., 2007; Misra et al., 2009; Frisoni et al., 2010).

In particular, hippocampal atrophy has emerged as an independent risk factor of progress towards dementia (Jack et al., 1999; Kantarci et al., 2009; Risacher et al., 2009; Frisoni et al., 2010). The hippocampus and entorhinal cortex suffer the earliest neuropathological changes of AD (Braak and Braak, 1991), and the ensuing hippocampal neurodegeration may be more directly linked to cognitive and clinical decline than other features of the pathological process (Price et al., 2001; Savva et al., 2009; Jack et al., 2008). Longitudinal studies have indicated that MCI subjects destined to convert towards dementia have reduced hippocampal volume relative to non-converters (Kantarci et al., 2009; Risacher et al., 2009).

* Corresponding author at: Institute of Psychiatry, King's College London, De Crespigny Park, PO Box 89, London SE5 8AF, UK. Fax: +44 203 228 2016.
*E-mail address:* sergi.1.costafreda@kcl.ac.uk (S.G. Costafreda).
[1] The AddNeuroMed Consortium.

1053-8119/$ – see front matter © 2011 Elsevier Inc. All rights reserved.
doi:10.1016/j.neuroimage.2011.01.050

Three-dimensional shape analysis can pinpoint the precise localization of early hippocampal atrophy (Csernansky et al., 2005; Apostolova et al., 2006; Morra et al., 2009). Shape analysis may therefore provide more accurate prognostic predictions of cognitive decline than hippocampal volume, as already suggested using manual expert segmentation (Ferrarini et al., 2009; Frisoni et al., 2010). Manual segmentation, however, is highly resource intensive and is not scalable to routine clinical use. Developing a fully automated approach able to capitalize on the predictive potential of hippocampal shape abnormalities for prognostic prediction would be a key step towards clinical application. In the present study, we sought to investigate to what extent 3D hippocampal shape abnormalities predicted 1-year conversion to overt AD and cognitive decline in individuals with MCI. We employed an automated segmentation technique, which has been validated in AD (Morra et al., 2008), to ensure efficient and consistent hippocampal measurements in a large sample. We applied a novel mapping algorithm (Shi et al., 2009) to transform the segmented hippocampi into 3D shapes with one-to-one point correspondence across subjects to permit direct inter-subject statistical analysis. This algorithm models the intrinsic geometric properties of each hippocampus and thus achieves a correspondence robust to variations in orientation or position of the hippocampus across subjects.

From the AddNeuroMed multisite study (Lovestone et al., 2007; Simmons et al., 2009, 2011), 103 amnestic MCI subjects with baseline and 1-year neuroimaging and behavioral assessments were investigated. We hypothesized that those MCI subjects already expressing at baseline a hippocampal atrophic phenotype that is compatible with AD would suffer an accelerated cognitive decline and would be more likely to convert to dementia than those not presenting with this atrophic phenotype. To test this hypothesis, we used the baseline scans of 71 AD and 88 age-matched healthy controls (HC) from the same study to develop a classifier trained to separate AD from HC individuals based on hippocampal shape. The trained classifier can therefore be seen as an accurate detector of the atrophic phenotype characteristic of AD. We then inputed the baseline morphometric features for each MCI individual into the trained classifier and received for each subject a label as to whether the atrophic phenotype characteristic of AD was present or not at the beginning of the follow-up in a given MCI individual. To test whether this phenotypic labeling was valuable for prognostic prediction, we then compared the clinical and cognitive 1-year outcome of MCI individuals with and without the atrophic phenotype. In addition to this individual classification analysis, we employed a conventional group analysis to reveal the hippocampal subregions most associated with conversion to AD and cognitive decline.

The shape-based predictive model was developed using Support Vector Machine (SVM) (Vapnik, 2000) classification, which has been shown to be a powerful tool for statistical pattern recognition in neuroimaging-based clinical prediction (Davatzikos et al., 2005; Fu et al., 2008; Fan et al., 2008b; Kloppel et al., 2008; Vemuri et al., 2008; Costafreda et al., 2009; Nouretdinov et al., in press). For comparison purposes, we also trained a volume-based SVM model, with the expectation that shape-based models would result in superior prediction accuracy of conversion to AD.

## Methods

### *Participants and behavioral assessment*

AddNeuroMed is a longitudinal, multisite study of biomarkers for AD (Lovestone et al., 2007), recruiting subjects from six European sites. Ethical approval was obtained at each data acquisition site, and informed consent was obtained for all subjects (Table 1). Control subjects were aged 65 years or above, in good general health and had a baseline Mini Mental State Examination (MMSE, (Tombaugh and McIntyre, 1992)) score higher than 24. Subjects with MCI had subjective memory impairment and a score below 1.5 SD of population age-adjusted norms on the Consortium to Establish a Registry for Alzheimer's Disease cognitive battery (CERAD, (Welsh et al., 1994)), a score of 0.5 on the Clinical Dementia Rating scale (CDR, (Hughes et al., 1982)), an MMSE score above 24 and did not have any functional impairments. Subjects with AD were recruited as defined by both NINCDS–ADRDA criteria for mild to moderate AD (McKhann et al., 1984) and DSM-IV criteria for probable AD. AD subjects also had an MMSE score range between 12 and 28, Hachinski Modified Ischemic (HMI, (Hachinski et al., 1975)) score of at most 4 and a Global Deterioration Scale (GDS, (Reisberg et al., 1982)) score between 2 and 5. Clinical assessments included a detailed case and family history, the CDR, HMI, MMSE, GDS and CERAD cognitive battery, the latter only for MCI and HC subjects. General exclusion criteria were neurological or psychiatric disease other than AD, significant unstable systemic illness or organ failure, and alcohol or substance misuse. Recruited subjects underwent MRI scanning, with follow-up assessments at 3 and 12 months.

**Table 1**
Demographic and clinical characteristic of the participants.

| | MCI ($N=103$) | | HC ($N=88$) | | AD ($N=71$) | |
|---|---|---|---|---|---|---|
| | Mean | SD | Mean | SD | Mean | SD |
| Demographics | | | | | | |
| Age | 74.1 | 5.8 | 73.6 | 6.7 | 74.9 | 5.8 |
| Female sex (No. %) | 51 | 51 | 46 | 52 | 50 | 70 |
| Years of education | 9 | 4.3 | 10.6 | 4.8 | 7.6 | 4 |
| Clinical measures | | | | | | |
| Baseline | | | | | | |
| CDR score | 0.5 | 0 | 0 | 0 | 1.3 | 0.6 |
| GDS score | 2.3 | 0.5 | 1 | 0 | 3.7 | 0.8 |
| MMSE score | 27.1 | 1.7 | 29.1 | 1.2 | 21.1 | 4.6 |
| CERAD delayed recall* | 3.9 | 2 | 6.5 | 2.1 | | |
| Change at 12 months | | | | | | |
| Diagnostic changes (No.%) | 22 | 21% | 0 | 0 | 0 | 0 |
| MMSE score | −1.2 | 4 | −0.2 | 1.3 | −1.7 | 6.2 |
| CERAD delayed recall* | −0.4 | 1.9 | 0.5 | 1.8 | | |
| Volume ($cm^3$) | | | | | | |
| Right hippocampus | 4.1 | 0.6 | 4.3 | 0.5 | 3.8 | 0.6 |
| Left hippocampus | 3.9 | 0.5 | 4.1 | 0.4 | 2.5 | 0.6 |

MCI: mild cognitive impairment, HC: healthy controls, AD: Alzheimer's disease. *: AD subjects were not assessed using the CERAD battery. All diagnostics changes were conversions from MCI to AD.

In the present report, we included those MCI and control subjects who had satisfactorily completed their baseline and 12-month behavioral assessment, resulting in a final sample of 103 MCI, 71 ADC and 88 HC1. At follow-up, the clinical diagnosis of 22 of the MCI subjects was changed to AD, according to NINCDS–ADRDA criteria (McKhann et al., 1984). This binary measure of clinical deterioration was complemented by two continuous measures: change in MMSE score between baseline and 12 months as an estimate of general cognitive decline and the change in delayed recall test score of the CERAD battery as a specific measure of memory function (Welsh et al., 1991) dependent on hippocampal integrity (Kramer et al., 2004).

### *MR data acquisition and pre-processing*

The neuroimaging protocol was designed for compatibility with the Alzheimer's disease Neuroimaging Initiative (ADNI) magnetic resonance (MR) protocol and has been presented in detail previously (Jack et al., 2008; Simmons et al., 2009, 2011). Briefly, MR data were obtained from six 1.5 T MR systems with a standardized protocol, including quality assurance and control. The present report is based on high resolution sagittal 3D MP-RAGE scans acquired at baseline with full brain and skull coverage, optimized for morphometric analyses. After reconstruction, in-plane resolution was $256\times256$ with in-plane voxel size of $0.9375\times0.9375$ mm and slice thickness of

1.2 mm. Pre-processing was performed with the FreeSurfer software suite (Fischl et al., 2002). Images were interpolated to an isotropic voxel size of 1 $mm^3$, and their intensity was normalized using the automated N3 algorithm (Sled et al., 1998), followed by skull stripping and neck removal (Segonne et al., 2004; Fischl et al., 2002). The skull stripped brain images were the input for the automated hippocampal segmentation.

*Automated hippocampal segmentation and mapping*

Automated hippocampal segmentation was performed using a pattern recognition algorithm designed for use in AD studies and validated on data from the ADNI study (Morra et al., 2008). Briefly, the pattern recognition algorithm was trained on a sample of "ground truth," manually segmented hippocampi of 21 representative subjects (7 AD, 7 MCI and 7 healthy controls) from the ADNI data set, produced following a standardized segmentation protocol (http://cms.loni.ucla.edu/ncrr/protocol.aspx?id=732). The pattern recognition algorithm itself implements an auto-context model that learns a classification rule for hippocampal vs nonhippocampal voxels based on a large set of local image features extracted from the ground truth segmented brains, such as image intensity, position and curvatures (Tu and Bai, 2010; Morra et al., 2008). Segmented outputs of the algorithm have been shown to be in good agreement with independent hippocampal segmentations produced by human experts (Morra et al., 2008).

An initial 3D mesh representation of each hippocampus was constructed based on the segmented images. Direct hippocampal mapping (Shi et al., 2007, 2009) was then used to map this initial mesh representation into a common triangulation with one-to-one vertex correspondence across all subjects, thus making possible the between-subject local-shape statistical analysis. To achieve this correspondence, DHM models the intrinsic geometric properties of each hippocampus and thus achieves a correspondence robust to variations in orientation or position of the hippocampus across subjects.

Intrinsic local radial distances, reflecting the distance between a point in the common triangulation and a medial core of the hippocampus, were employed as the features for both conventional group analysis and patient classification. A simple interpretation for radial distance can be given as the "thickness" of the hippocampus at that particular point. Direct comparisons between radial distances at analogous points between subjects can be made, and a reduction in radial distance can be interpreted as evidence of atrophy. In the intrinsic approach presented by Shi et al. (2009), the medial core is defined as a 3D curve characterizing the geometric tail-to-head trend of the hippocampus. This curve is obtained from a general shape modeling approach, appropriate for elongated structures, and crucially, it is intrinsic in the sense that it is completely defined by the shape of the hippocampus. In particular, determining this intrinsic medial core does not necessitate any *a priori* sectioning of the hippocampus (Thompson et al., 2004). It is therefore robust to differences in the position and orientation of the hippocampus across subjects. The raw intrinsic radial distance, computed in the subject's native brain space, was normalized for global head size effects using the cube-root of the total intracranial volume as computed by FreeSurfer. This normalized intrinsic radial distance measure was then used for between-subject statistical shape analysis. We also produced a normative atlas for display purposes by averaging the hippocampal-mapped surfaces of the healthy subjects.

*Conventional analysis of group differences in volume and shape analysis*

We used general linear modeling (GLM) to study the effects of clinical status at 12 months (MCI converters vs non-converters) and changes in score between baseline and follow-up for the continuous variables (MMSE and CERAD-recall) on normalized hippocampal volume and radial distance. Covariates of no interest were age, sex and baseline scores. Continuous variables were standardized before model estimation. When mapping the association between hippocampal shape and the variables of interest, we fitted independent models at each vertex (2000 models in total for each statistical map). Multiple comparisons correction was performed by permutation testing using a set-level statistic, namely the number of vertices whose $t$-value for the covariate of interest survived an initial uncorrected threshold of $p<0.01$ (Friston et al., 1996). The experimental statistic obtained from the observed map was then compared to a permutation-driven $t$-distribution. This $t$-distribution was generated under the null hypothesis of no association between local radial distance and the variable of interest by permuting the values of the predicted variable across subjects, refitting the model with the permuted labels and re-computing the statistic for the covariate of interest (Anderson and Robinson, 2001). We used 10,000 iterations of this permutation procedure to test the overall statistical significance of the statistical maps. Statistical significance was set at a unilateral $\alpha=0.05$ reflecting the hypothesis that reduced volume and radial distance would be associated with cognitive decline (clinical conversion, MMSE score decrease and CERAD delayed recall score decrease). The interpretation of these set-level corrected $p$-values is whether it is likely to find such an extensive pattern of association between atrophy in the hippocampus and a given variable by chance alone. If the corrected $p$-value is less than 0.05, then the whole pattern of association can be declared statistically significant. We refer to evidence for atrophy at the level of whole hippocampal pattern as "3D shape atrophy." This procedure differs from simply testing volumetric differences in that in the 3D shape atrophy procedure we introduce the belief that the atrophy does not occur uniformly throughout the hippocampus, but rather, there are some areas where atrophy initiated earlier or is faster. The set level procedure can then focus on these areas with more extreme change (which we identify through the initial thresholding procedure at $p<0.01$, uncorrected), and if the assumption of focalised changes is correct, then the 3D shape atrophy test should be more sensitive than a simple volumetric procedure, where atrophic reduction in some areas may be dampened by the relative lack of atrophy in the rest of the hippocampus.

*Classification analysis*

Classification analysis was conducted using Support Vector Machines (SVM) (Vapnik, 2000), which have demonstrated optimal empirical results in neuroimaging-based applications (Davatzikos et al., 2005; Fu et al., 2008; Fan et al., 2008a; Kloppel et al., 2008; Costafreda et al., 2009; Nouretdinov et al., in press). Briefly, SVM treats the measurements from a given individual as a single point in a multidimensional space, with the number of dimensions being, in our application, the number of vertices for left and right hippocampus. The location of the point representing a subject in this space is determined by the normalized intrinsic radial distance at each vertex. SVM finds an optimal separation (the maximal margin separating hyperplane) between points belonging to different classes (e.g. AD vs HC) after mapping the original features via a kernel function. The position of the separating hyperplane is entirely defined by those data instances closest to the group boundaries, the so-called support vectors. The kernel function may be linear, in which case the optimal separation is a hyperplane defined in the original feature space, or it may be non-linear, leading to non-linear separation of classes in the original space. Following previous applications in AD (Ferrarini et al., 2009; Misra et al., 2009), we chose the non-linear Gaussian radial basis kernel as it affords more modeling flexibility, which can lead to better performance. The downside of this flexibility is that non-linear separation may result in model overfitting. In our application, the risk of overfitting was reduced by the relatively large sample sizes

available for model training ($N = 159$) and the fact that the test set of MCI subjects was completely independent from the training samples.

A binary classification model was trained to distinguish AD from HC subjects. We computed the four-fold cross-validated diagnostic accuracy, to assess to what extent this approach identified the atrophic phenotype associated with AD. Then, the model was trained with the full training sample of AD and HC subjects and applied to the shape data from the MCI subjects. Each MCI individual was categorized as AD or HC shape phenotype, and this prediction was compared with the 1-year clinical outcomes. Permutation testing with 10,000 random allocations of class membership was used to assess the statistical significance of the difference in conversion rate between MCI subjects with and without the atrophic phenotype and of the accuracy in predicting conversion. Repeated-measures analysis of variance (ANOVA) was also employed to assess the statistical significance in the differential rate of cognitive decline between both groups of MCI subjects. To visualize the discriminative shape patterns, we employed a recently described approximate method (Koutsouleris et al., 2009) whereby pairs of support vectors from opposite classes with the minimum distance across the separating hyperplane are selected to compute a set of "nearest neighbor" difference vectors, which are then averaged to create the discriminative shape pattern. Throughout the analysis, the SVM parameter $C$ was fixed to 1. Image preprocessing, automated segmentation and 3D mapping were performed using the LONI Pipeline (Dinov et al., 2009), while GLM analysis and SVM classification were conducted using R (http://cran.r-project.org/).

## Results

### *Conventional group analysis*

MCI subjects who converted to AD experienced faster cognitive decline than non-converters: the 1-year decline of MMSE score was of 5.0 points in converters and 0.2 points in non-converters (repeated-measures ANOVA time-by-group interaction test: $p<0.001$), and the 1-year decline in CERAD delayed recall score was of 1.1 points in converters and 0.2 points in non-converters ($p<0.01$).

Those MCI subjects who later converted to AD showed a smaller baseline volume right (9.2%, $p<0.0001$) and left (6.7%, $p<0.0035$) hippocampi (Table 2). Reduced hippocampal volume was also correlated with memory decline bilaterally as measured by CERAD delayed recall, while the association with decline in cognitive performance as measured by the MMSE score was not statically significant.

Three-dimensional shape analysis showed that bilateral focal hippocampal atrophy at baseline was associated with MCI clinical conversion to AD (Table 3, Fig. 1a). Hippocampal thinning was distributed in the left and right hippocampal head and body, with the most intense changes localized in the right hippocampal head. Bilateral focal hippocampal atrophy was also associated with subsequent decline in CERAD scores (Fig. 1b), while right hippocampal atrophy was linked to subsequent deterioration in MMSE scores (Fig. 1c).

**Table 2**
Association of baseline hippocampal volume to clinical conversion to Alzheimer's disease and cognitive decline at 12 months in subjects with mild cognitive impairment.

| | Right | | Left | |
|---|---|---|---|---|
| | % atrophy | *p*-value | % atrophy | *p*-value |
| Clinical conversion: MCI to AD | −9.2 | <0.0001 | −6.7 | 0.0035 |
| Correlation to verbal memory (CERAD delayed recall) | −3.0 | 0.0019 | −1.7 | 0.0092 |
| Correlation to MMSE total score | −1.2 | 0.1420 | −0.9 | 0.2094 |

Atrophy is the percent decrease in volume in converters from mild cognitive impairment to Alzheimer's disease or, for the continuous variables, the percent volume change associated with a subsequent decrease of 1 standard deviation in the scores. The *p*-value is the unilateral test for the association between atrophy in volume and subsequent changes in the variable of interest.

**Table 3**
Association of baseline hippocampal 3D shape atrophy to clinical conversion to Alzheimer's disease and cognitive decline at 12 months in subjects with mild cognitive impairment.

| | Right *p*-value | Left *p*-value |
|---|---|---|
| Clinical conversion: MCI to AD | <0.0001 | 0.0072 |
| Correlation to verbal memory (CERAD delayed recall) | 0.0018 | 0.0052 |
| Correlation to MMSE total score | 0.0101 | 0.1206 |

The *p*-values have been corrected for multiple comparisons using a set-level procedure (see Methods).

### *Individual classification analysis*

Prognostic prediction for MCI subjects was based on a Support Vector Machine (SVM) classification model trained to discriminate AD patients from healthy controls based on their baseline hippocampal morphometric features. This model identified the diagnostic category of AD and HC subjects with an accuracy of 85% ($p<0.0001$). The discriminative shape pattern pointed to bilateral atrophy in lateral

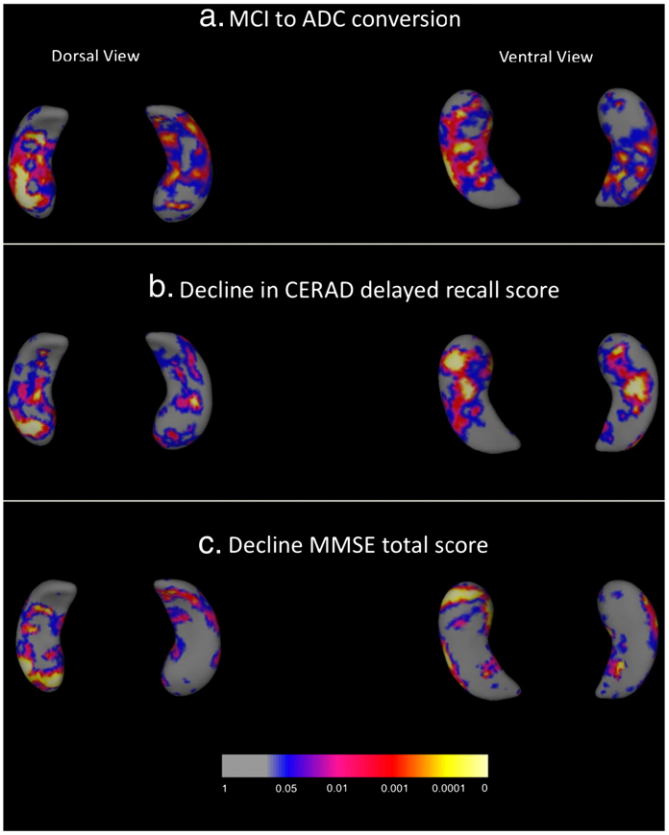


**Fig. 1.** Statistical significance maps for a) differences in atrophy between subjects with mild cognitive impairment who developed Alzheimer's disease (AD) within 12 months of follow-up ($N = 22$) and those who did not ($N = 81$); b) correlation in MCI subjects between atrophy and 12-month memory decline as measured by the CERAD delayed recall score ($N = 103$) and c) correlation between atrophy and MMSE total score ($N = 103$). The maps are adjusted for age, sex, baseline score (CERAD and MMSE) and intracranial volume. While the maps represent uncorrected *p*-values for local atrophy, a significant effect remained after multiple comparison correction at the set-level through permutation testing, except for the association between left hippocampal atrophy and MMSE score. Figures are in radiological convention (left is right).

and medial aspects of hippocampal head and to a lesser extent in hippocampal body as phenotypic features of AD (Fig. 2).

This model was then used for individualized prognostic prediction in the MCI sample (Table 4). MCI subjects with a pattern of hippocampal atrophy suggestive of AD at baseline demonstrated a statistically significant higher rate of conversion to AD of 52% at 1-year (17 converters out of 33 MCI subjects with the baseline AD atrophic phenotype) as compared to those subjects who did not express the baseline phenotype, who had a conversion rate of 7% (only 5 converters out of 70 MCI subjects without the baseline atrophic phenotype; test for equality of proportions $p<0.0001$). Those MCI subjects with the atrophic phenotype at baseline also suffered from faster cognitive deterioration in MMSE scores (ANOVA time-by-group interaction test: $p<0.01$, Fig. 3) and CERAD verbal memory ($p<0.01$), although their baseline scores were not significantly different ($p<0.3$ in both cases). Overall, the shape-based model predicted conversion to AD with 80% accuracy (the probability of achieving this accuracy by chance was $p<0.0001$) (Table 4).

For comparison purposes, another SVM model was also trained following identical procedures but based on bilateral volumetric measures; although this model was also accurate (74%, $p<0.001$, Table 4), it did not reach the same performance as the prognostic prediction based on 3D hippocampal morphology.

**Table 4**
Prognostic classification performance for the prediction of conversion to Alzheimer's disease in subjects with mild cognitive impairment based on 3D shape analysis and volume of both hippocampi.

| | Shape | Volume |
|---|---|---|
| True positive | 17 | 16 |
| True negative | 65 | 60 |
| False positive | 16 | 21 |
| False negative | 5 | 6 |
| Sensitivity, % | 77 | 73 |
| Specificity, % | 80 | 74 |
| PPV, % | 52 | 43 |
| NPV, % | 93 | 91 |
| Accuracy, % | 80 | 74 |
| Model significance | <0.0001 | 0.0008 |

PPV: positive predictive value, NPV: negative predictive value. Model significance was computed through 10000 random permutations of the prognostic outcomes (conversion to Alzheimer's disease or no conversion; see Methods).

## Discussion

Baseline hippocampal morphology measured by automated methods accurately predicted 1 year progression towards dementia in MCI subjects. MCI subjects with and without the AD hippocampal phenotype at baseline were not distinguishable by neuropsychological measures in general cognitive or memory function. However, the MRI-identified MCI subjects with the AD phenotype at baseline showed a substantially higher rate of conversion to AD and accelerated cognitive decline as compared to MCI subjects without the AD phenotype.

These findings suggest that hippocampal morphological analysis may offer added prognostic value relative to standard clinical and neuropsychological evaluation. As the prognostic test was developed and tested in different clinical samples (AD and HC for development, MCI for testing), these findings are likely to be robust and may be generalizable to other clinical settings. The clinical applicability of our approach is greatly enhanced by using an automated procedure for hippocampal extraction, thus achieving reproducible and user-independent measurements, validated against expert manual segmentation in a similar population (Morra et al., 2008) and efficiently scalable to large samples.

Such a prognostic test could have clinical applications, for example by encouraging watchful waiting in an individual with MCI identified as low-risk but more active clinical management which may include pharmacological interventions in an MCI subject at high-risk for developing AD. Our study followed the MCI subjects for 12 months, and it is likely that prognostic prediction of conversion to AD based on pre-existing atrophy is most accurate for MCI subjects within this relatively short period (Frisoni et al., 2010; Risacher et al., 2009). Prediction of imminent transition may be particularly useful for clinical trial enrichment, whereby test positive subjects could be selectively included with the expectation of transition within the time frame of a typical disease modification trial in ADs, which is rarely much longer than 12 months (Lovestone et al., 2007). This strategy increases the proportion of patients who could benefit from the intervention and optimizes the statistical power of the trial (Kohannim et al., in press; Frisoni et al., 2010).

The accuracy of the prediction of conversion to AD reached 80% (sensitivity = 77%, specificity = 80%), which is in the top range of previously published results of prognostic classification using structural neuroimaging (Table 5; Teipel et al., 2007; Ferrarini et al., 2009; McEvoy et al., 2009; Misra et al., 2009; Plant et al., 2010; Duchesne et al., 2010). It is noticeable that the studies that used only hippocampal shape ((Ferrarini et al., 2009), and the present paper) achieved a predictive performance comparable or superior to those employing a multi-region or whole brain approach (Teipel et al., 2007; McEvoy et al., 2009; Misra et al., 2009; Plant et al., 2010; Duchesne et al., 2010). This finding is in accordance with the early involvement of the hippocampus in the neuropathological pathway leading to AD (Braak and Braak, 1991). Hippocampal atrophy also has the largest effect size across brain areas for the differentiation of stable and progressive MCI (Risacher et al., 2009). We found that volumetric measures alone resulted in inferior prognostic performance relative to shape analysis. The same finding was verified by Ferrarini et al. (2009)

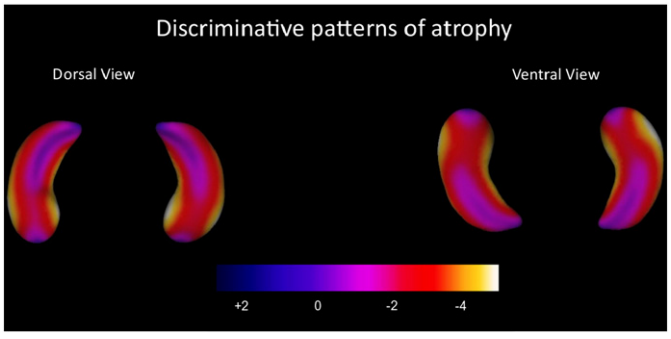


**Fig. 2.** Hippocampal shape pattern discriminative between Alzheimer's disease (AD) and healthy controls, which was also predictive of the risk of transition to AD in subjects with mild cognitive impairment. Negative numbers represent atrophy in AD subjects. Figure in radiological convention (left is right).

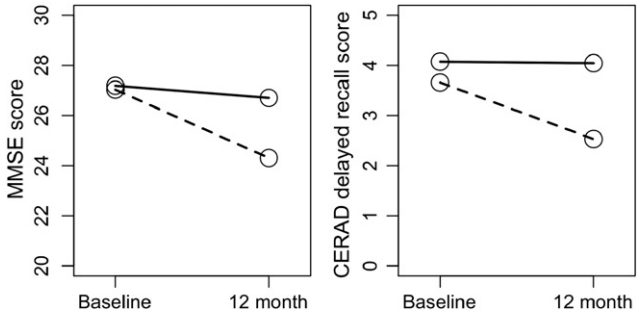


**Fig. 3.** Subjects with mild cognitive impairment predicted to develop Alzheimer's disease based on their hippocampal morphometry ($N=33$, dashed lines) show faster decline over the 12 month follow-up in both verbal memory (CERAD delayed memory scores, $p<0.01$) and general cognitive function (MMSE total score, $p<0.01$) than MCI subjects predicted to remain stable ($N=70$, solid lines).

**Table 5**
Selected recent literature on the prognostic capacity of structural neuroimaging for the prediction of conversion to Alzheimer's disease in subjects with mild cognitive impairment.

| Study | Data type | Region | Converters/total MCI | Follow-up (months) | Classifier | Training | Test | Acc | Se | Sp |
|---|---|---|---|---|---|---|---|---|---|---|
| Ferrarini et al., 2009 | Shape (manual) | Hippocampus | 15/30 | 33 | nSVM | MCI | C-V | 80 | 80 | 80 |
| | Volume (manual) | Hippocampus | 15/30 | 33 | nSVM | MCI | C-V | 73 | 63 | 77 |
| McEvoy et al., 2009 | Volume (semi-auto) | Multi-region[a] | 33/160 | 12 | ROC | AD + HC | MCI | 58 | 79 | 52 |
| Teipel et al., 2007 | VBM (CSF) | Whole Brain | 9/24 | 27 | ROC + LR | AD + HC | MCI | 80 | 67 | 93 |
| Misra et al., 2009 | VBM (GM and WM) | Whole Brain | 27/103 | 15 | nSVM | MCI | C-V | 75–80 | NR | NR |
| Duchesne et al., 2010 | local VBM-like[b] | Medial Temp | 11/31 | 28 | LD | AD + HC | C-V | 81 | 70 | 100 |
| Plant et al., 2010 | VBM (GM) | Whole Brain | 9/24 | 30 | VFI | AD + HC | MCI | 75 | 56 | 87 |
| **Weighted Average** | | | | | | | | **74** | **72** | **76** |
| Present study | Shape (automated) | Hippocampus | 22/103 | 12 | nSVM | AD + HC | MCI | 80 | 77 | 80 |

Acc: accuracy; Se: sensitivity; Sp: specificity; VBM: voxel-based morphometry; CSF: Cerebrospinal fluid; GM: grey matter; WM: white matter; ROC: receiver operating characteristic; LR: logistic regression; nSVM: non-linear support vector machines classification; VFI: voting feature interval; LD: linear discriminant; C-V: cross-validation; NR: not reported. Only those studies which reported prognostic accuracy in a separate sample (the test sample) from that used to develop the prognostic model (the training sample) were included; the testing sample may consist of fully independent subjects or may have been obtained through cross-validation (leaving aside a part of the training sample for testing). The average performance metrics were obtained by weighting each individual study results by their sample size.

[a] Regions of interest included mesial and lateral temporal, isthmus cingulate and orbitofrontal areas.

[b] Duchesne et al., 2010 employed as classification features the image intensity and local volume change in a medial temporal ROI.

based on manual hippocampal segmentation. In general, we observe that prognostic prediction based on detailed morphometric pattern analysis generally outperformed those based on summary measures such as volume (Table 5), suggesting that detailed three-dimensional atrophy analysis of hippocampus may be an optimal approach for prognosis in MCI subject (Frisoni et al., 2010).

Several strategies could further improve the accuracy of prognostic prediction. The entorhinal cortex is affected by the neuropathological changes leading to AD at least as early as the hippocampus (Hyman et al., 1984; Braak and Braak, 1991; Frisoni et al., 2006; Frisoni et al., 2010). The addition of entorhinal atrophy could therefore increase prognostic performance relative to the analysis of hippocampal changes alone (Dickerson et al., 2001).

Additionally, previous 3D morphometric studies on changes associated with future cognitive decline have pointed to atrophy in similar hippocampal subregions as those reported here. Csernansky et al. (2005) followed a sample of 49 individuals for an average of 5 years, demonstrating significant inward deformation of the hippocampal head and lateral left surface (approximately identified as the cornus ammonis 1 or CA1 subfield) between 14 subjects who converted from CDR 0 to 0.5 and those that did not. Apostolova et al. (2006) studied 20 MCI subjects during 3 years, of which 6 later developed AD (converters), 7 reverted to a normal cognitive level (improvers) and 7 remained diagnosed with MCI (stable). Although there were no significant differences between converters and stable subjects, there were bilateral shape differences between converters and improvers, identified in the CA1 and subiculum subregions. Using the ADNI data set ($N = 243$ MCI subjects), Morra et al. (2009) found an association between atrophy in lateral and medial aspects of the right hippocampus, particularly in the hippocampal head, and future decline in CDR Sum-of-Boxes scores.

In our sample, the most intense atrophy preceding cognitive decline and conversion in MCI subjects was also located in the right hippocampal head, particularly in its lateral aspect, with less prominent atrophy extending to more posterior regions. Additionally, the discriminative pattern of atrophy of the SVM classifier, predictive of clinical decline in MCI subjects, also showed an antero-posterior gradient in atrophy, with the most intense changes located in the lateral and medial aspects of hippocampal head. The convergence between our findings (using both group analysis and pattern classification) and the existing literature (Csernansky et al., 2005; Apostolova et al., 2006; Morra et al., 2009) strongly suggests that hippocampal head atrophy may be an early warning sign of risk of conversion to Alzheimer. Although our automated procedure segments the whole of the hippocampus, thus preventing the attribution of changes to definite regions or subfields, our findings are broadly compatible with early anterior CA1 involvement as defined in previous studies (Csernansky et al., 2005; Apostolova et al., 2006; Malykhin et al., 2010). Focusing on these early changes may further increase the sensitivity of a prognostic probe.

Our group analyses also suggested that right hippocampus may suffer from earlier and more intense atrophy than its left counterpart. In contrast, the discriminative pattern of atrophy was strongly symmetrical. While both strategies offer unbiased populational estimates, the discriminative pattern is based on larger, clearly separable and more balanced samples (AD vs healthy controls) than the group analyses which are dependent on the relatively low number of MCI subjects who converted to AD. These optimal statistical properties of the AD vs healthy controls discriminative pattern should lead to reduced statistical noise and therefore more reliable results relative to the group contrasts, a feature that is apparent in the smoother appearance of the discriminative pattern (Fig. 2). The symmetry of the discriminative pattern therefore suggests that the increased atrophy in right hippocampus apparent in our group results could be a feature of our particular MCI sample rather than a fact generalizable to the population. Replication in an independent sample would be desirable to further explore the existence of potential asymmetry.

The diagnosis of MCI conversion towards probable dementia of the Alzheimer type was based on widely used clinical and neuropsychological criteria (McKhann et al., 1984). These criteria do not rely on MRI scanning, and therefore the classification accuracy reported here is unbiased. However, a limitation of our study is that the diagnosis was based on these clinical criteria and not verified through pathology. Hippocampal atrophy alone may not be a specific marker of AD and may also occur in other dementia types (de Leon et al., 2007). Rather, hippocampal atrophy, which correlates to neuronal loss, may be a sensitive marker of cognitive and clinical deterioration, with a more direct link to clinical decline than other neuropathological changes (Savva et al., 2009; Mormino et al., 2009; Jack et al., 2010). Hippocampal shape analysis may therefore be profitably combined with additional biomarkers linked to other specific AD processes, such as amyloidal deposition, that could provide complementary information (de Leon et al., 2006; Bouwman et al., 2007; Jack et al., 2008; Jack et al., 2009; Hansson et al., 2009; Driscoll et al., in press), leading to a precise staging of the neuropathological pathway leading to AD.

## Acknowledgments

Work supported by the National Institute for Health Research (NIHR) Specialist Biomedical Research Centre for Mental Health award to the South London and Maudsley NHS Foundation Trust and the Institute of Psychiatry, King's College London. This work was

partially funded by the National Science Foundation grant 0716055, the National Institutes of Health through the NIH Roadmap for Medical Research, grant U54 RR021813, and AddNeuroMed has received financial support from the European Community under the FP6.

## References


Anderson, M., Robinson, J., 2001. Permutation tests for linear models. Aust. N Z J. Stat. 43 (1), 75–88.

Apostolova, L.G., Dutton, R.A., Dinov, I.D., Hayashi, K.M., Toga, A.W., Cummings, J.L., Thompson, P.M., May 2006. Conversion of mild cognitive impairment to Alzheimer disease predicted by hippocampal atrophy maps. Arch. Neurol. 63 (5), 693–699.

Bouwman, F., Schoonenboom, S., van Der Flier, W., Van Elk, E., Kok, A., Barkhof, F., Blankenstein, M., Scheltens, P., 2007. CSF biomarkers and medial temporal lobe atrophy predict dementia in mild cognitive impairment. Neurobiol. Aging 28 (7), 1070–1074.

Braak, H., Braak, E., 1991. Neuropathological stageing of Alzheimer-related changes. Acta Neuropathol. 82 (4), 239–259.

Costafreda, S.G., Chu, C., Ashburner, J., Fu, C.H.Y., 2009. Prognostic and diagnostic potential of the structural neuroanatomy of depression. PLoS ONE 4 (7), e6353.

Csernansky, J.G., Wang, L., Swank, J., Miller, J.P., Gado, M., McKeel, D., Miller, M.I., Morris, J.C., Apr 2005. Preclinical detection of Alzheimer's disease: hippocampal shape and volume predict dementia onset in the elderly. Neuroimage 25 (3), 783–792.

Davatzikos, C., Shen, D., Gur, R., Wu, X., Liu, D., Fan, Y., Hughett, P., Turetsky, B., Gur, R., 2005. Whole-brain morphometric study of schizophrenia revealing a spatially complex set of focal abnormalities. Arch. Gen. Psychiatry 62 (11), 1218–1227.

de Leon, M.J., Mosconi, L., Blennow, K., DeSanti, S., Zinkowski, R., Mehta, P.D., Pratico, D., Tsui, W., Saint Louis, L.A., Sobanska, L., Brys, M., Li, Y., Rich, K., Rinne, J., Rusinek, H., Feb 2007. Imaging and CSF studies in the preclinical diagnosis of Alzheimer's disease. Ann. NY Acad. Sci. 1097, 114–145.

de Leon, M.J., DeSanti, S., Zinkowski, R., Mehta, P.D., Pratico, D., Segal, S., Rusinek, H., Li, J., Tsui, W., Saint Louis, L.A., Clark, C.M., Tarshish, C., Li, Y., Lair, L., Javier, E., Rich, K., Lesbre, P., Mosconi, L., Reisberg, B., Sadowski, M., DeBernadis, J.F., Kerkman, D.J., Hampel, H., Wahlund, L.-O., Davies, P., Mar 2006. Longitudinal CSF and MRI biomarkers improve the diagnosis of mild cognitive impairment. Neurobiol. Aging 27 (3), 394–401.

Dickerson, B., Goncharova, I., Sullivan, M., Forchetti, C., Wilson, R., Bennett, D., Beckett, L., deToledo Morrell, L., 2001. MRI-derived entorhinal and hippocampal atrophy in incipient and very mild Alzheimer's disease. Neurobiol. Aging 22 (5), 747–754.

Dinov, I.D., Van Horn, J.D., Lozev, K.M., Magsipoc, R., Petrosyan, P., Liu, Z., Mackenzie-Graham, A., Eggert, P., Parker, D.S., Toga, A.W., 2009. Efficient, distributed and interactive neuroimaging data analysis using the LONI pipeline. Front Neuroinformatics 3, 22.

Driscoll, I., Zhou, Y., An, Y., Sojkova, J., Davatzikos, C., Kraut, M., Ye, W., Ferrucci, L., Mathis, C., Klunk, W., Wong, D., Resnick, S., Feb 2010. Lack of association between (11)C-PiB and longitudinal brain atrophy in non-demented older individuals. Neurobiol Aging. In Press.

Duchesne, S., Bocti, C., De Sousa, K., Frisoni, G., Chertkow, H., Collins, D., 2010. Amnestic MCI future clinical status prediction using baseline MRI features. Neurobiol. Aging 31, 1606–1617.

Fan, Y., Batmanghelich, N., Clark, C., Davatzikos, C., 2008a. Spatial patterns of brain atrophy in MCI patients, identified via high-dimensional pattern classification, predict subsequent cognitive decline. Neuroimage 39 (4), 1731–1743.

Fan, Y., Resnick, S., Wu, X., Davatzikos, C., 2008b. Structural and functional biomarkers of prodromal Alzheimer's disease: a high-dimensional pattern classification study. Neuroimage 41 (2), 277–285.

Ferrarini, L., Frisoni, G., Pievani, M., Reiber, J., Ganzola, R., Milles, J., 2009. Morphological hippocampal markers for automated detection of Alzheimer's disease and mild cognitive impairment converters in magnetic resonance images. J. Alzheimers Dis. 17 (3), 643–659.

Fischl, B., Salat, D.H., Busa, E., Albert, M., Dieterich, M., Haselgrove, C., van der Kouwe, A., Killiany, R., Kennedy, D., Klaveness, S., Montillo, A., Makris, N., Rosen, B., Dale, A.M., Jan 2002. Whole brain segmentation: automated labeling of neuroanatomical structures in the human brain. Neuron 33 (3), 341–355.

Frisoni, G., Sabattoli, F., Lee, A., Dutton, R., Toga, A., Thompson, P., 2006. In vivo neuropathology of the hippocampal formation in AD: a radial mapping MR-based study. Neuroimage 32 (1), 104–110.

Frisoni, G., Fox, N., Jack, C., Scheltens, P., Thompson, P., 2010. The clinical use of structural MRI in Alzheimer disease. Nat. Rev. Neurol. 6 (2), 67–77.

Friston, K.J., Holmes, A., Poline, J.B., Price, C.J., Frith, C.D., Dec 1996. Detecting activations in PET and fMRI: levels of inference and power. Neuroimage 4 (3 Pt 1), 223–235.

Fu, C.H.Y., Mourao-Miranda, J., Costafreda, S.G., Khanna, A., Marquand, A.F., Williams, S. C.R., Brammer, M.J., 2008. Pattern classification of sad facial processing: toward the development of neurobiological markers in depression. Biol. Psychiatry 63 (7), 656–662.

Hachinski, V., Iliff, L., Zilhka, E., Du Boulay, G., McAllister, V., Marshall, J., Russell, R., Symon, L., 1975. Cerebral blood flow in dementia. Arch. Neurol. 32 (9), 632.

Hansson, O., Buchhave, P., Zetterberg, H., Blennow, K., Minthon, L., Warkentin, S., 2009. Combined rCBF and CSF biomarkers predict progression from mild cognitive impairment to Alzheimer's disease. Neurobiol. Aging 30 (2), 165–173.

Hughes, C.P., Berg, L., Danziger, W.L., Coben, L.A., Martin, R.L., Jun 1982. A new clinical scale for the staging of dementia. Br. J. Psychiatry 140, 566–572.

Hyman, B.T., Hoesen, G.W.V., Damasio, A.R., Barnes, C.L., 1984. Alzheimer's disease: cell-specific pathology isolates the hippocampal formation. Science 225 (4667), 1168–1170.

Jack Jr., C., Petersen, R., Xu, Y., O'Brien, P., Smith, G., Ivnik, R., Boeve, B., Waring, S., Tangalos, E., Kokmen, E., 1999. Prediction of AD with MRI-based hippocampal volume in mild cognitive impairment. Neurology 52 (7), 1397.

Jack Jr., C., Knopman, D., Jagust, W., Shaw, L., Aisen, P., Weiner, M., Petersen, R., Trojanowski, J., 2010. Hypothetical model of dynamic biomarkers of the Alzheimer's pathological cascade. Lancet Neurol. 9 (1), 119–128.

Jack, C.R.J., Bernstein, M.A., Fox, N.C., Thompson, P., Alexander, G., Harvey, D., Borowski, B., Britson, P.J., LWhitwell, J., Ward, C., Dale, A.M., Felmlee, J.P., Gunter, J.L., Hill, D.L. G., Killiany, R., Schuff, N., Fox-Bosetti, S., Lin, C., Studholme, C., DeCarli, C.S., Krueger, G., Ward, H.A., Metzger, G.J., Scott, K.T., Mallozzi, R., Blezek, D., Levy, J., Debbins, J.P., Fleisher, A.S., Albert, M., Green, R., Bartzokis, G., Glover, G., Mugler, J., Weiner, M.W., Apr 2008. The Alzheimer's Disease Neuroimaging Initiative (ADNI): MRI methods. J. Magn. Reson. Imaging 27 (4), 685–691.

Jack, C.R.J., Lowe, V.J., Senjem, M.L., Weigand, S.D., Kemp, B.J., Shiung, M.M., Knopman, D.S., Boeve, B.F., Klunk, W.E., Mathis, C.A., Petersen, R.C., Mar 2008. 11C PiB and structural MRI provide complementary information in imaging of Alzheimer's disease and amnestic mild cognitive impairment. Brain 131 (Pt 3), 665–680.

Jack, C.R.J., Lowe, V.J., Weigand, S.D., Wiste, H.J., Senjem, M.L., Knopman, D.S., Shiung, M.M., Gunter, J.L., Boeve, B.F., Kemp, B.J., Weiner, M., Petersen, R.C., May 2009. Serial PIB and MRI in normal, mild cognitive impairment and Alzheimer's disease: implications for sequence of pathological events in Alzheimer's disease. Brain 132 (Pt 5), 1355–1365.

Kantarci, K., Weigand, S.D., Przybelski, S.A., Shiung, M.M., Whitwell, J.L., Negash, S., Knopman, D.S., Boeve, B.F., O'Brien, P.C., Petersen, R.C., Jack, C.R.J., Apr 2009. Risk of dementia in MCI: combined effect of cerebrovascular disease, volumetric MRI, and 1H MRS. Neurology 72 (17), 1519–1525.

Killiany, R.J., Hyman, B.T., Gomez-Isla, T., Moss, M.B., Kikinis, R., Jolesz, F., Tanzi, R., Jones, K., Albert, M.S., Apr 2002. MRI measures of entorhinal cortex vs hippocampus in preclinical AD. Neurology 58 (8), 1188–1196.

Kloppel, S., Stonnington, C., Chu, C., Draganski, B., Scahill, R., Rohrer, J., Fox, N., Jack, C., Ashburner, J., Frackowiak, R., 2008. Automatic classification of MR scans in Alzheimer's disease. Brain 131 (3), 681.

Kohannim, O., Hua, X., Hibar, D., Lee, S., Chou, Y.Y., Toga, A.W., Jack, C.R., Weiner, M.W., Thompson, P.M., 2010. Boosting power for clinical trials using classifiers based on multiple biomarkers. Neurobiol Aging 31 (8), 1429–1442.

Koutsouleris, N., Meisenzahl, E., Davatzikos, C., Bottlender, R., Frodl, T., Scheuerecker, J., Schmitt, G., Zetzsche, T., Decker, P., Reiser, M., et al., 2009. Use of neuroanatomical pattern classification to identify subjects in at-risk mental states of psychosis and predict disease transition. Arch. Gen. Psychiatry 66 (7), 700.

Kramer, J.H., Schuff, N., Reed, B.R., Mungas, D., Du, A.-T., Rosen, H.J., Jagust, W.J., Miller, B. L., Weiner, M.W., Chui, H.C., Jul 2004. Hippocampal volume and retention in Alzheimer's disease. J. Int. Neuropsychol. Soc. 10 (4), 639–643.

Lovestone, S., Francis, P., Strandgaard, K., 2007. Biomarkers for disease modification trials—the innovative medicines initiative and AddNeuroMed. J. Nutr. Health Aging 11 (4), 359–361 Jul-Aug.

Malykhin, N., Lebel, R., Coupland, N., Wilman, A., Carter, R., 2010. In vivo quantification of hippocampal subfields using 4.7 T fast spin echo imaging. Neuroimage 49 (2), 1224–1230.

McEvoy, L., Fennema-Notestine, C., Roddey, J., Hagler, D., Holland, D., Karow, D., Pung, C., Brewer, J., Dale, A., 2009. Alzheimer disease: quantitative structural neuroimaging for detection and prediction of clinical and structural changes in mild cognitive impairment. Radiology 251 (1), 195–205.

McKhann, G., Drachman, D., Folstein, M., Katzman, R., Price, D., Stadlan, E.M., Jul 1984. Clinical diagnosis of Alzheimer's disease: report of the NINCDS–ADRDA Work Group under the auspices of Department of Health and Human Services Task Force on Alzheimer's Disease. Neurology 34 (7), 939–944.

Misra, C., Fan, Y., Davatzikos, C., Feb 2009. Baseline and longitudinal patterns of brain atrophy in MCI patients, and their use in prediction of short-term conversion to AD: results from ADNI. Neuroimage 44 (4), 1415–1422.

Mormino, E., Kluth, J., Madison, C., Rabinovici, G., Baker, S., Miller, B., Koeppe, R., Mathis, C., Weiner, M., Jagust, W., 2009. Episodic memory loss is related to hippocampal-mediated β-amyloid deposition in elderly subjects. Brain 132 (5), 1310–1323.

Morra, J.H., Tu, Z., Apostolova, L.G., Green, A.E., Avedissian, C., Madsen, S.K., Parikshak, N., Hua, X., Toga, A.W., Jack, C.R.J., Weiner, M.W., Thompson, P.M., 2008. Validation of a fully automated 3D hippocampal segmentation method using subjects with Alzheimer's disease, mild cognitive impairment, and elderly controls. Neuroimage 43 (1), 59–68.

Morra, J.H., Tu, Z., Apostolova, L.G., Green, A.E., Avedissian, C., Madsen, S.K., Parikshak, N., Hua, X., Toga, A.W., Jack, C.R.J., Schuff, N., Weiner, M.W., Thompson, P.M., 2009. Automated 3D mapping of hippocampal atrophy and its clinical correlates in 400 subjects with Alzheimer's disease, mild cognitive impairment, and elderly controls. Hum. Brain Mapp. 30 (9), 2766–2788.

Nelson, P.T., Braak, H., Markesbery, W.R., 2009. Neuropathology and cognitive impairment in Alzheimer disease: a complex but coherent relationship. J. Neuropathol. Exp. Neurol. 68 (1), 1–14.

Nouretdinov, I., Costafreda, S., Gammerman, A., Chervonenkis, A., Vovk, V., Vapnik, V., Fu, C., May 2010. Machine learning classification with confidence: application of transductive conformal predictors to MRI-based diagnostic and prognostic markers in depression. Neuroimage. In Press. doi:10.1016/j.neuroimage.2010.05.023.

Petersen, R., Doody, R., Kurz, A., Mohs, R., Morris, J., Rabins, P., Ritchie, K., Rossor, M., Thal, L., Winblad, B., 2001. Current concepts in mild cognitive impairment. Arch. Neurol. 58 (12), 1985.

Plant, C., Teipel, S.J., Oswald, A., Böhm, C., Meindl, T., Mourao-Miranda, J., Bokde, A.W., Hampel, H., Ewers, M., 2010. Automated detection of brain atrophy patterns based on MRI for the prediction of Alzheimer's disease. NeuroImage 50 (1) 162–174.

Price, J.L., Ko, A.I., Wade, M.J., Tsou, S.K., McKeel, D.W., Morris, J.C., Sep 2001. Neuron number in the entorhinal cortex and CA1 in preclinical Alzheimer disease. Arch. Neurol. 58 (9), 1395–1402.

Reisberg, B., Ferris, S.H., de Leon, M.J., Crook, T., Sep 1982. The Global Deterioration Scale for assessment of primary degenerative dementia. Am. J. Psychiatry 139 (9), 1136–1139.

Risacher, S.L., Saykin, A.J., West, J.D., Shen, L., Firpi, H.A., McDonald, B.C., Aug 2009. Baseline MRI predictors of conversion from MCI to probable AD in the ADNI cohort. Curr. Alzheimer Res. 6 (4), 347–361.

Savva, G.M., Wharton, S.B., Ince, P.G., Forster, G., Matthews, F.E., Brayne, C., May 2009. Age, neuropathology, and dementia. N. Engl. J. Med. 360 (22), 2302–2309.

Segonne, F., Dale, A.M., Busa, E., Glessner, M., Salat, D., Hahn, H.K., Fischl, B., Jul 2004. A hybrid approach to the skull stripping problem in MRI. Neuroimage 22 (3), 1060–1075.

Shi, Y., Morra, J.H., Thompson, P.M., Toga, A.W., 2009. Inverse-consistent surface mapping with Laplace–Beltrami eigen-features. Inf. Process Med. Imaging 21, 467–478.

Shi, Y., Thompson, P.M., de Zubicaray, G.I., Rose, S.E., Tu, Z., Dinov, I., Toga, A.W., Sep 2007. Direct mapping of hippocampal surfaces with intrinsic shape context. Neuroimage 37 (3), 792–807.

Simmons, A., Westman, E., Muehlboeck, S., Mecocci, P., Vellas, B., Tsolaki, M., Kloszewska, I., Wahlund, L.-O., Soininen, H., Lovestone, S., Evans, A., Spenger, C., the AddNeuroMed consortium, 2011. The AddNeuroMed framework for multi-centre MRI assessment of Alzheimer's disease: experience from the first 24 months. Int. J. Ger. Psych. 26, 75–82.

Simmons, A., Westman, E., Muehlboeck, S., Mecocci, P., Vellas, B., Tsolaki, M., Kloszewska, I., Wahlund, L.-O., Soininen, H., Lovestone, S., Evans, A., Spenger, C., Oct 2009. MRI measures of Alzheimer's disease and the AddNeuroMed study. Ann. NY Acad. Sci. 1180, 47–55.

Sled, J.G., Zijdenbos, A.P., Evans, A.C., Feb 1998. A nonparametric method for automatic correction of intensity nonuniformity in MRI data. IEEE Trans. Med. Imaging 17 (1), 87–97.

Teipel, S., Born, C., Ewers, M., Bokde, A., Reiser, M., Möller, H., Hampel, H., 2007. Multivariate deformation-based analysis of brain atrophy to predict Alzheimer's disease in mild cognitive impairment. Neuroimage 38 (1), 13–24.

Thompson, P.M., Hayashi, K.M., De Zubicaray, G.I., Janke, A.L., Rose, S.E., Semple, J., Hong, M.S., Herman, D.H., Gravano, D., Doddrell, D.M., Toga, A.W., Aug 2004. Mapping hippocampal and ventricular change in Alzheimer disease. Neuroimage 22 (4), 1754–1766.

Tombaugh, T.N., McIntyre, N.J., Sep 1992. The Mini-Mental State Examination: a comprehensive review. J. Am. Geriatr. Soc. 40 (9), 922–935.

Tu, Z., Bai, X., 2010. Auto-context and its application to high-level vision tasks and 3D brain image segmentation. IEEE T Pattern Anal. 32 (10) 1744–1757.

Vapnik, V., 2000. The nature of statistical learning theory. Springer Verlag.

Vemuri, P., Gunter, J., Senjem, M., Whitwell, J., Kantarci, K., Knopman, D., Boeve, B., Petersen, R., Jack Jr., C., 2008. Alzheimer's disease diagnosis in individual subjects using structural MR images: validation studies. Neuroimage 39 (3), 1186–1197.

Welsh, K.A., Butters, N., Mohs, R.C., Beekly, D., Edland, S., Fillenbaum, G., Heyman, A., Apr 1994. The Consortium to Establish a Registry for Alzheimer's Disease (CERAD). Part V. A normative study of the neuropsychological battery. Neurology 44 (4), 609–614.

Welsh, K., Butters, N., Hughes, J., Mohs, R., Heyman, A., Mar 1991. Detection of abnormal memory decline in mild cases of Alzheimer's disease using CERAD neuropsychological measures. Arch. Neurol. 48 (3), 278–281.